CENTER ROUTING SLIP

FROM	DATE
TSSG/RED	3 February 70

TO		INITIALS	DATE
DIRECTOR	5		
DEP/DIRECTOR	4		2/9
EXEC/DIRECTOR			
SPECIAL ASST	3	M	2/9
ASST TO DIR			
ASST TO DEP/DIR			
CH/PPBS			
DEP CH/PPBS			
EO/PPBS			
CH/IEG			
DEP CH/IEG			
EO/IEG			
CH/PSG			
DEP CH/PSG			
EO/PSG			
TSSG/RED	1		4 Feb
CH/TSSG	2		2/9
DEP CH/TSSG			
EO/TSSG			
CH/SSD/TSSG			
PERSONNEL			
LOGISTICS			
TRAINING			
RECORDS MGT			
SECURITY			
FINANCE			
DIR/IAS/DDI			
CH/DIAXX-4			
CH/DIAAP-9			
CH/[illegible]			

REMARKS

3-5 Reply to your query

Dr Z

John

I certainly agree with Dick on the resolution limitations of microwave radiometers. I know of this first hand since I developed such systems when at the DPSAT. I believe the primary application of such a technique is in the ERTS program – if the Center ever gets involved in exploiting their imagery then we really will have "to go to school" on the art of interpreting such imagery – It's got to complex yet similar to IR –

SECRET

R+D General

NPIC/TSSG/RED/SRB-007-70
3 February 1970

MEMORANDUM FOR THE RECORD

SUBJECT: Visit of [redacted] Personnel to NPIC

1. Per Mr. Lundahl's request, [redacted] 25X1
of [redacted] were invited to NPIC on 21 January 1970 to present a briefing on their microwave color imaging system.

2. The microwave radiometric instrumentation was developed by [redacted] 25X1
[redacted] under contract to NASA. The purpose of the system was to investigate the potential of microwave radiometry to earth resources, inventory and analysis. For this purpose, it may have some potential since it senses absolute differences in the thermal temperature (in Kelvins) of all objects on the earth's surfaces. It can do this in almost any type of weather and has the potential for real-time read-out. (See attached brochure)

3. The disadvantage of microwave radiometry for the foreseeable state-of-the-art is its gross ground resolution. The current system was designed to image a resolution element of 1,500' X 1,500' on the ground. Future development may reduce this to several hundred feet. Therefore, it has no apparent application for a reconnaissance imaging system (because of this gross resolution).

4. However, in discussing the general characteristics of microwave radiometry (other than for imaging of surface objects), a potential application to other high resolution reconnaissance system (photography) came to light as a possibility. It appears that microwave energy of a specified wavelength can "map" the top of cloud cover such as is done in the Nimbus weather satellite. Why, then, could not a small microwave radiometer cloud mapper be used to "trigger" a photographic system so that exposures would occur only in areas with very little cloud cover??? The [redacted] 25X1
people said that they had never considered that application, but that "off-the-top-of-the-head," they saw no theoretical or practical reason why it would not work. Furthermore, it would only have to be a small (suitcase-size) black box requiring very little power. They appeared to be quite interested in looking into this type of application to see what all of the problems might be. They were told that NPIC could not fund such a study since it is not within our charter, but that other people in the community might have an interest. The meeting adjourned on this note.

[redacted] 25X1
Chief/SRB/RED/TSSG

1/14

MEMORANDUM FOR: JWC

Obtained attached from ADM [redacted] today. Do we have any interest in [redacted] system? Let's discuss. If so, maybe one of the contract engineers could look it and report to us.

DATE

25X1

LUNDAHL

see p. 13

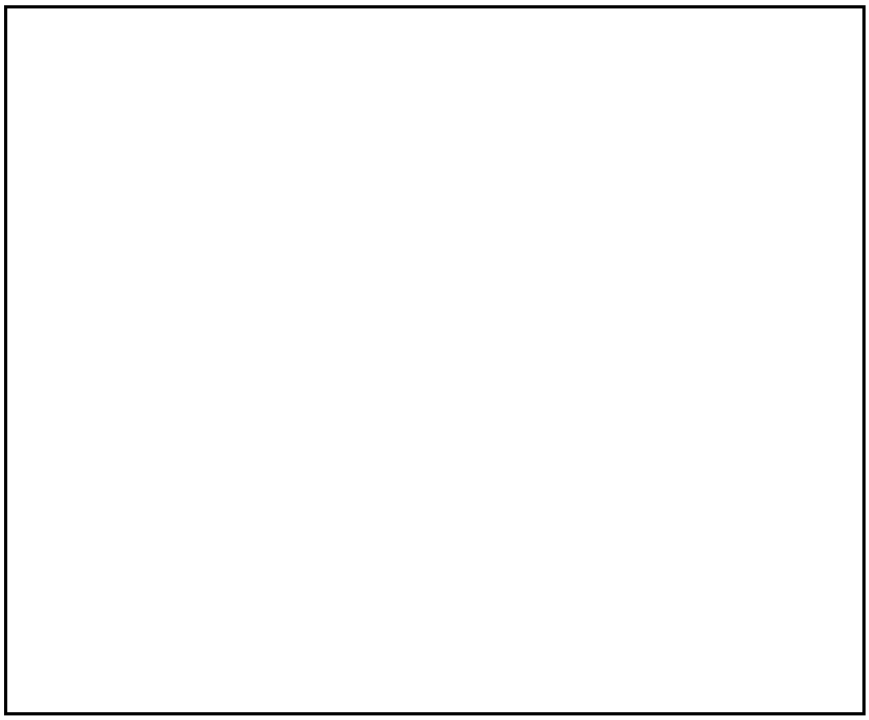

14th ANNUAL TECHNICAL SYMPOSIUM

Proceedings Reprint

MICROWAVE RADIOMETRIC INSTRUMENTATION FOR REMOTE SENSING APPLICATIONS

AUGUST 11 -14, 1969

25X

MICROWAVE RADIOMETRIC INSTRUMENTATION FOR REMOTE SENSING APPLICATIONS

INTRODUCTION

Remote sensing of objects by means of their thermal radiation is a well established technique. To date, thermal radiation imaging has primarily employed the infrared spectrum from 1 to 10 microns.

The subject of this presentation is radiometric imaging of terrestrial surfaces by sensing the thermal radiation at centimeter wavelengths. This wavelength region extending from .3 cm to 30 cm constitutes the microwave spectrum. At these wavelengths, which are very long compared to optical wavelengths, the radiation is relatively immune to scattering attenuation by fog and clouds. This property of microwave radiation is demonstrated by the successful all-weather operation of microwave radar systems. It provides the basis for all-weather radiometric imaging systems. An additional significant feature is that at these wavelengths radiation from terrestrial surfaces provides distinctive signatures not observable in the infrared and visual spectrum.

Recent advances in microwave solid state technology have resulted in the practical realization of airborne sensors providing real time microwave radiometric images of the underlying terrain. Figure 1 shows a strip map of the Southern California coastal region made from an altitude of 40,000 feet, by a radiometric imager operating at a wavelength of 1.55 cm. This image faithfully reveals the coast line and major geographical features. It was achieved in the presence of heavy haze and cloud cover. A significant feature of this map characteristic of radiometric imaging is the pronounced contrast of river basins, lakes and reservoirs. This image achieved by a first generation imager is indicative of the potentials for remote sensing application of microwave radiometric imaging.

The following discussion will describe the physical principles, instrumentation techniques and some of the remote sensing applications together with further examples of recent results.

MICROWAVE THERMAL RADIATION

The apparent intensity of the radiation originating at the surface of an object is in actuality the sum of two radiation components. One of these is the thermal radiation emitted from a body as a consequence of its finite temperature. The second component results from the reflection of illuminating radiation from a variety of sources. A perfect black body absorbs and emits radiation with a 100% effectiveness. It will not reflect incident illumination. Hence, a black body has an apparent radiation intensity dependent solely on its thermometric temperature. A perfect mirror is an example of the complementary situation where the surface brightness is dependent only upon the incident illuminating radiation. Most commonly occurring surfaces are not perfect black bodies or mirrors and consequently present a mixture of emission and reflection.

In observations of the earth's surface from airborne or satellite platforms the reflected radiation originates from the sky. In the absence of an atmosphere, the incident mircrowave radiation from the sky is the isotropic background radiation from outer space. A more significant source of incident radiation occurs in the presence of atmosphere as a consequence of its re-radiation. This re-radiation of the atmosphere is directly related to the atmospheric absorption.

EMISSION

At centimeter wavelengths and for terrestrial surface temperatures the emitted radiation intensity may be described by the Rayleigh-Jeans Law; namely, a direct linear dependence upon the thermometric temperature of the emitting body. This is illustrated by Figure 2, which shows black body radiation intensity distribution.

The ability of a surface to emit or absorb radiation in comparison to a perfect black body is termed the emissivity ϵ. The emitted radiation intensity is then conveniently characterized by an effective brightness temperature, T_b.

Emitted Radiation: $T_b = \epsilon(\lambda)\, T_h$ (1)

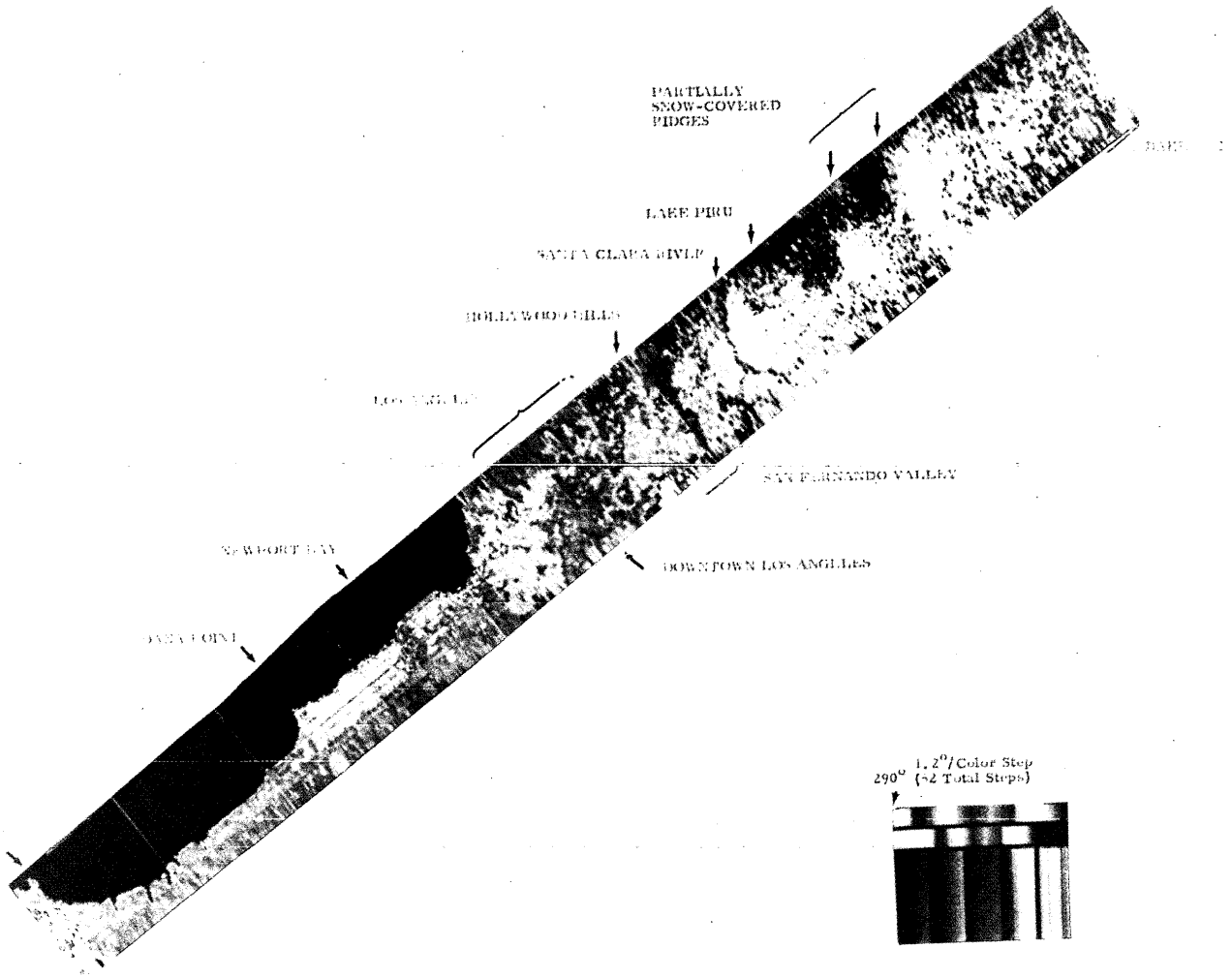

Figure 1. Relative Map of Terrain

Approved For Release 2004/02/11 : CIA-RDP78B05703A000100070021-5

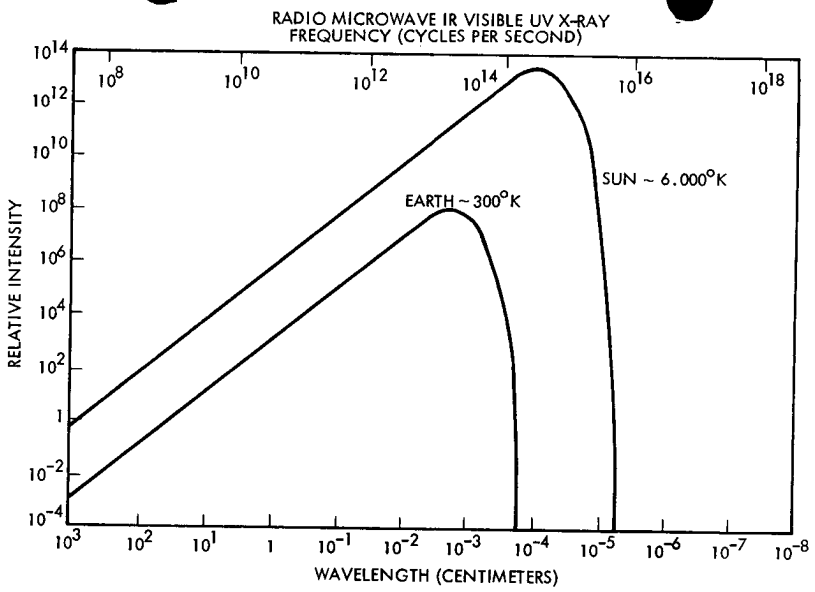

Figure 2. Black Body Radiation

T_b = The brightness temperature of the surface, i.e., the equivalent thermometric temperature of a black body.

$\epsilon(\lambda)$ = The emissivity of the surface at a given wavelength λ.

T_h = The thermometric temperature of the observed body.

The expression for brightness temperature in Equation (1) takes into account only the emitted radiation.

It is important to note that at microwave wavelengths the emissivities of materials are, in general, quite different from the values at infrared wavelengths. Even more significant at microwaves, are the much greater differences in the emissivities of various natural surfaces.

The contrasts within an image formed by microwave thermal radiation are primarily the result of different emissivities of the various constituents of the observed scene. In the microwave spectrum thermometric temperature differences contribute to radiometric images only in a secondary fashion. This represents a marked distinction from the infrared spectrum where the image is determined primarily by thermometric temperature differences.

Microwave radiation from most surfaces includes contributions originating at depths of several wavelengths. Clearly then, centimeter wavelength radiation from surfaces is much less dependent upon thermometric temperatures at the surface than is the case for infrared. Thús, microwave radiometric images are less subject to diurnal variations and atmospheric cooling.

Factors influencing the emissivities of surfaces are summarized in Table 1. The reflectivity of a surface may be described as the complement of its emissivity.

Table 1

FACTORS GOVERNING EMISSIVITIES

1) Wavelength
2) Complex Dielectric Constant $\epsilon' + j\,\epsilon''$
3) Complex Permeability $\mu' + j\,\mu''$
4) Surface Roughness
5) Angle of Incidence
6) Subsurface Reflections
7) Polarization

The total radiation from the surface may then be described in terms which include reflectivity, r, and a brightness temperature, $T_{sky}\ (\lambda,\phi)$, characterizing the intensity of the incident radiation from the sky at zenith angle, θ.

Total radiation:

$$T_b = \epsilon(\lambda,\theta)\, T_h + r\, T_{sky}\ (\lambda,\theta) \qquad (2\text{-a})$$

The above equation describes the microwave thermal radiation from a typical terrain surface element. The configuration is illustrated in Figure 3.

In general, the sky temperature is a function of wavelength and zenith angle. However, the proper selection of operating wavelengths within the microwave spectrum T_{sky} values of less than $30^{o}K$ are achieved. Hence, typically $T_h \geq 270^{o}K$, and $T_{sky} \ll T_h$.

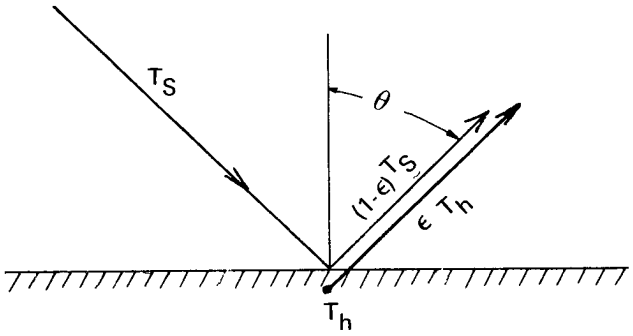

$$T_b = \epsilon T_h + (1-\epsilon) T_S$$

Where:

T_b = terrain brightness temp.

T_S = sky brightness temperature

T_h = surface thermometric temp.

ϵ = emissivity

$1-\epsilon$ = reflection coefficient

θ = incidence angle

Figure 3. Sources of Measured Radiation

Substituting for, r, in terms of $(1-\epsilon)$ an alternate form for T_b is

$$T_b = T_{sky}(\theta,\lambda) + \epsilon(\lambda,\theta)\left[T_h - T_{sky}(\theta,\lambda)\right] \quad (2\text{-}b)$$

The contrast in brightness temperature between two adjacent terrain elements viewed at the same wavelength and incidence angle as determined by their respective emissivities ϵ_1 and ϵ_2 is

$$T_{b2} - T_{b1} = (\epsilon_2 - \epsilon_1)(T_h - T_{sky}) \quad (2\text{-}c)$$

Where: it is assumed that $T_{h1} = T_{h2}$

It is evident that the magnitude of the available contrast in brightness temperatures generated by differences in surface emissivities is directly dependent on the difference between the thermometric temperature and the incident sky temperature at the surface. Clearly, progressive increase in T_{sky} as a consequence of increased atmospheric absorption results in a corresponding decrease in the available contrast at the originating surface.

ATMOSPHERIC TRANSMISSION

The attenuation (reciprocal transmittance) of the total path from the earth's surface to the top of the atmosphere is shown in Figure 4, for wavelengths ranging from 3 cm to 0.1 cm. The conditions include zero zenith angle and moderate to low relative humidity conditions. As indicated in the figure, the attenuation peaks centered at 22.235 and 60 GHz are associated with water vapor and oxygen, respectively. An additional attenuation term increasing monotonically with frequency is the scattering caused by condensed water droplets in form of fog, clouds, and rain. Clearly, this magnitude is dependent directly on the local weather. At frequencies below 30 GHz, i.e., wavelengths greater than 1 cm experimental investigations confirm theoretical predictions that only the most severe rain storms have any serious effects on microwave propagation through the atmosphere. (Ref. 1, 2). Typically, statistical data indicates 50% reduction in transmission occurring less than 0.5% of the total time. Even in these cases the microwave image is not totally obscured.

To minimize absorption effects of water vapor and oxygen, the wavelength regions most suitable for remote sensing of the earth's surface are "window bands" centered at 0.33 cm and 0.8 cm as well as the wavelengths greater than 1.5 cm. In normal weather conditions the effects of atmospheric absorption can be readily accounted for.

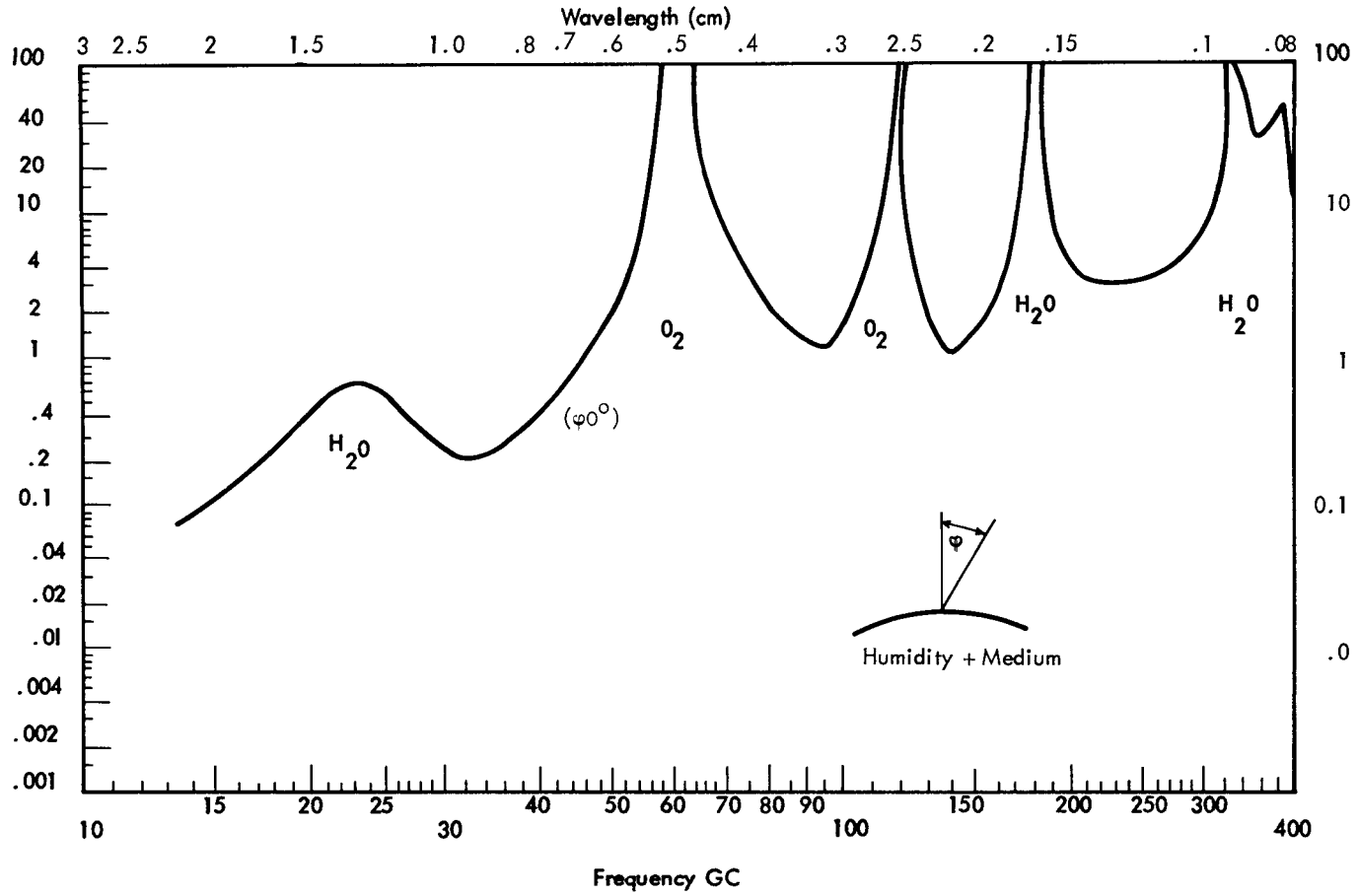

Figure 4. Atmospheric Attenuation in the Microwave and Millimeter Spectrum

The sky brightness temperature T_{sky} incident upon the earth's surface at a given incidence angle φ and wavelength λ is given by:

$$T_{sky} = \left[1 - t_o(\varphi,\lambda)\right] T_{atm} + 3.5^oK \qquad (3)$$

where T_{atm} is the average thermometric temperature of the total atmosphere. $t_o(\varphi,\lambda)$ is the total atmospheric transmission factor at a wavelength, λ, and an incidence angle φ. The 3.5^oK constant is the cosmic radiation background temperature. (Ref. 3).

This value of T_{sky} employed in Equation (2) yields the actual value of the apparent brightness temperature directly at the surface. The value of T_b is modified to a value T_b' at the airborne sensor.

$$T_b' = T_b\, t_\ell(\varphi,\lambda) + T_{atm}\left[1 - t_\ell(\varphi,\lambda)\right] \qquad (4)$$

Where t_ℓ is the atmospheric transmission factor of the path from the surface to the sensor

T_b is given by Equation (2)

TOTAL RADIATION FROM TYPICAL SURFACES

The radiation intensity received by the microwave radiometric sensor from a given surface element is completely characterized by Equation (2-4).

In a typical environment both the emissivity and the incident sky radiation are a function of incidence angle. The quantitative dependence of emissivity upon incidence angles is shown for a number of common materials in Figure 5.

It is apparent that natural and man-made surfaces present a large range of brightness temperatures. In particular, water surfaces and the presence of soil moisture generate very prominent contrasts.

In general, observations are conducted by detecting the horizontal component of radiation, however, some particularly interesting effects are observed by a simultaneous comparison of horizontal and vertical polarization. Some results shown in Figure 6 indicate that

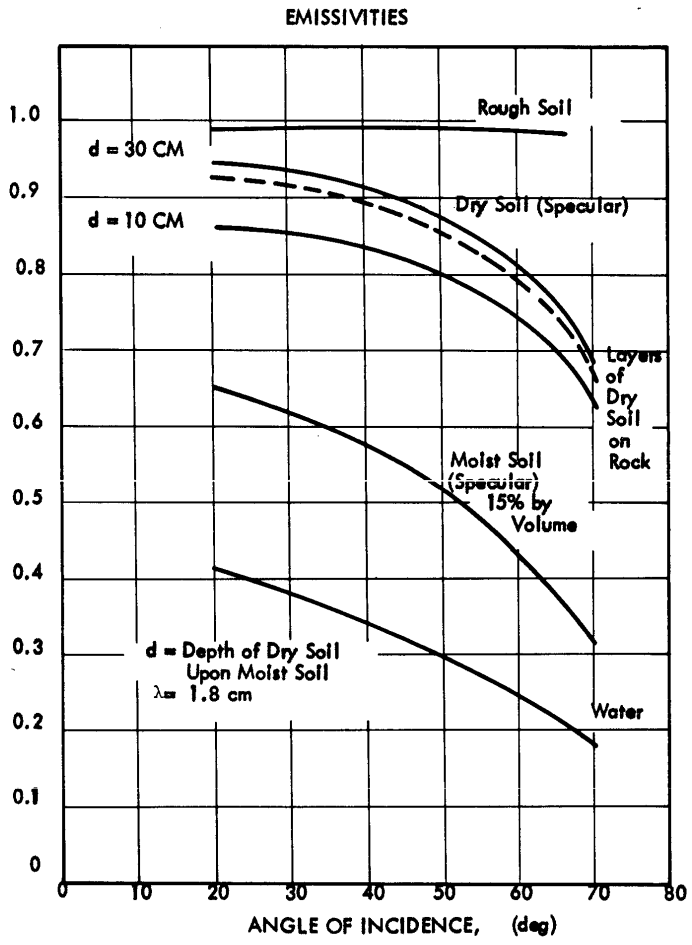

Figure 5. Emissivities of Natural Surfaces. (Horizontal Polarization)

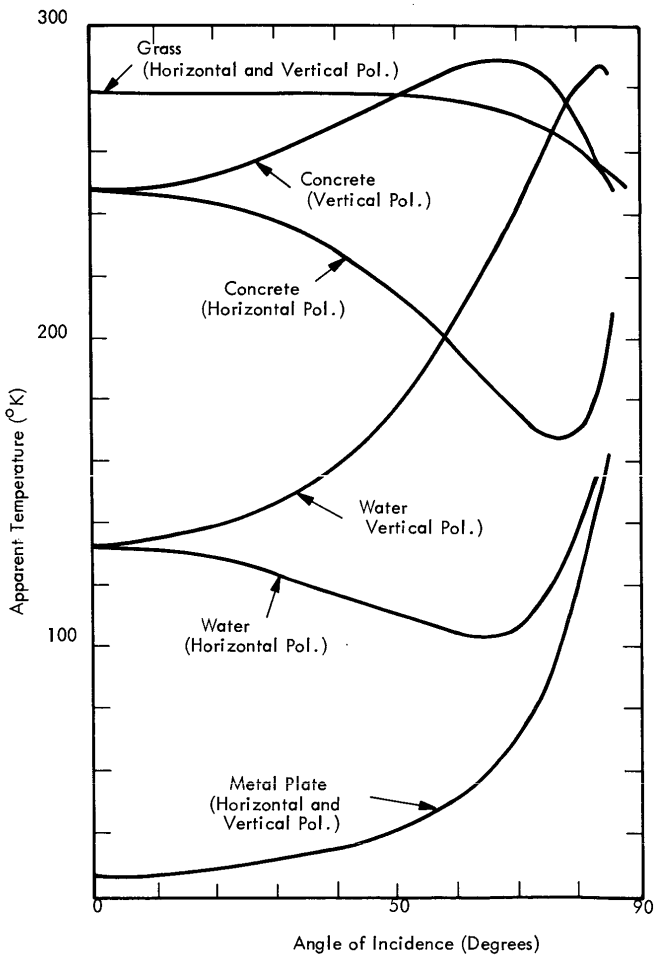

Figure 6. Horizontal and Vertical Polarization Apparent Temperatures of Surfaces at 19.4 GHz.

observation at incidence angles of approximately 50^{o} and comparison of the two polarizations provide a unique method of identifying the presence of small water bodies.

The further exploitation of the polarization differences has been suggested for a number of sea state applications.

The quantitative measurement of sea state by microwave brightness temperature observation has been proposed by Stogryn. (Ref. 4) Ocean brightness temperatures as a function of incidence angle and wind speed have been computed for both horizontal and vertical polarization. The results are plotted in Figure 7a and Figure 7b respectively. Examination of these results indicates that at an incidence angle of approximately 50^{o}, the vertical component of brightness temperature is essentially independent of sea state. The horizontally polarized component is strongly dependent upon the speed of the winds acting upon the ocean surface. This provides a potentially highly useful method of all-weather airborne surveillance of ocean surface state.

MICROWAVE RADIOMETRIC IMAGING SYSTEMS

BASIC RADIOMETER

The basic form of microwave radiometric receiver is shown in Figure 8. It is in many respects quite similar to infrared radiometer systems. The most significant difference is that the use of low noise predetection gain in the case of the microwave radiometer cause it to be considerably more sensitive than the best direct detection infrared instrument. This results in signal to noise ratio for microwave systems which equal or exceed those of infrared systems.

At microwaves the radiation collecting aperture can take a variety of forms ranging from simple mechanically pointed parabolic or cassegrain reflector arrangements to electronically scanned phased array antennas. The antenna may also be described as a transformer matching the impedance of three dimensional space to that of a transmission line feeding the input of the microwave receiver.

A matched antenna may be considered as having a radiation resistance equal to that of the receiver transmission line. In effect the antenna acts the same as a resistive termination. Nyquist has shown that the available power per unit bandwidth, P', from a resistive termination is:

$$P' = kT$$

Where: k = Boltzmann's constant

T = is the temperature of the termination

Matched transmission line terminations act in the same fashion as black bodies in that they emit incoherent radiation directly proportional to their thermometric temperature. In the case of an antenna acting as the termination of a transmission line, the apparent temperature of its radiation resistance is dependent upon the radiation it receives from the outside world. This temperature is referred to as the apparent temperature of the antenna. In the case of a perfect antenna with no dissinative internal losses, this apparent antenna temperature, T_a. is totally independent of the antenna structure temperature. (Ref. 5)

The brightness temperature characterization of the radiation from the observed body can be extended to that of antenna radiation temperature. The increase of antenna temperature T_a due to brightness temperature T_b' of an observed body is given by:

$$T_a = \frac{\Omega_b}{\Omega_a} \; T_b' \qquad (5)$$

Where

$\Omega_b = \frac{A}{4\pi d^2}$ is the solid angle subtended at the sensor by the observed object.

Ω_a is the solid angle of the antenna beam pattern.

A and d are respectively the area and distance of the observed body.

As indicated in Figure 8, the input to the microwave receiver input transmission line is periodically switched between the antenna and a reference black body at a known temperature T_r. This most frequently employed configuration was developed by Dicke in 1946. (Ref. 6) It was the advantages of ameliorating receiver gain stability problems as well as comparing the received

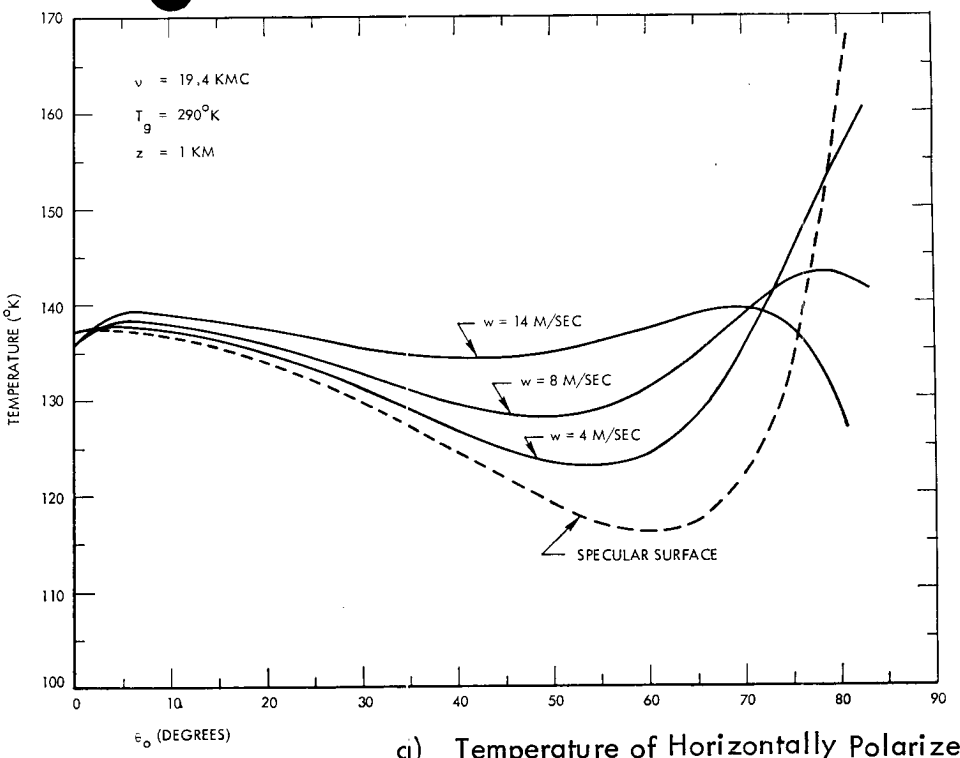

a) Temperature of Horizontally Polarized Radiation as a Function of Angle (Upwind Case).

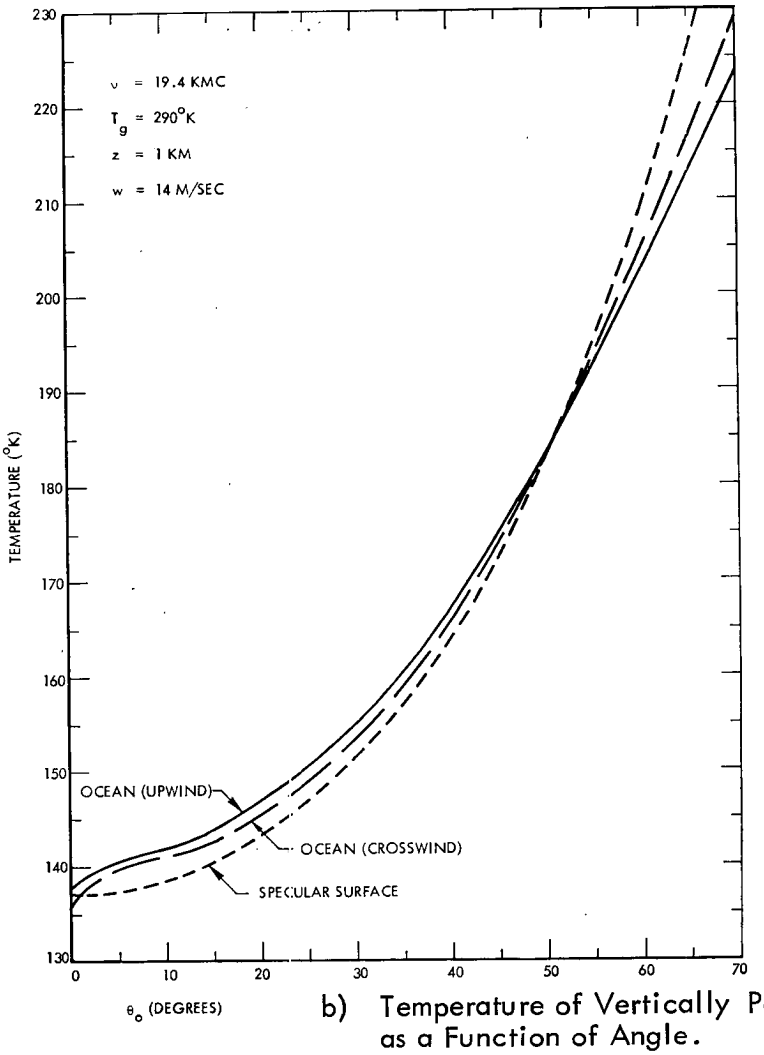

b) Temperature of Vertically Polarized Radiation as a Function of Angle.

Figure 7. Ocean Surface Apparent Temperatures

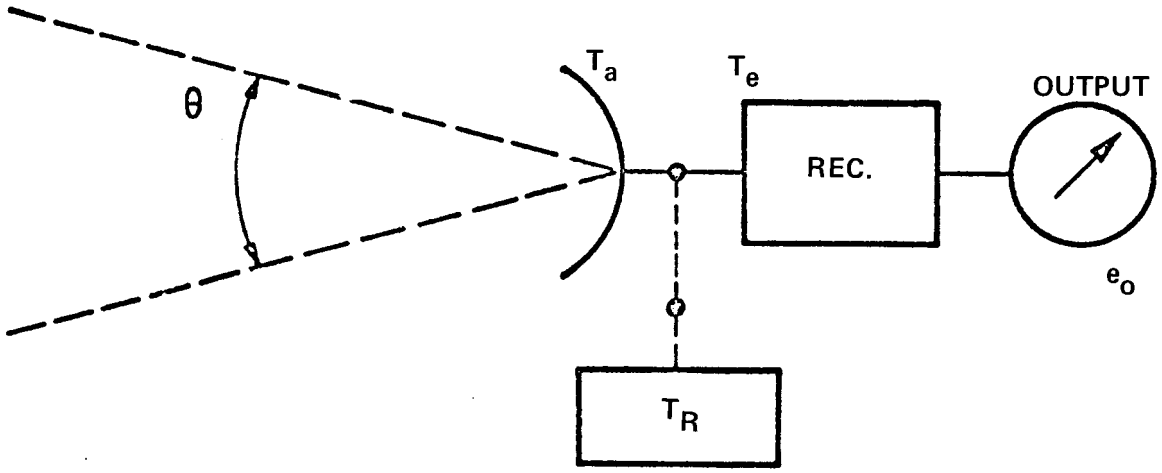

T_a = Antenna Temperature - Indicative of Received Thermal Radiation

T_R = Thermal Temperature of Radiation Reference Source

T_e = Equivalent Noise Temperature of Receiver - Indicative of the Thermal Noise Power Generated within Receiver - Competes Against Thermal Radiation Power from Antenna.

Figure 8. Basic Microwave Radiometer

radiation with a standard reference. The minimum detectable change in antenna temperature as determined by externally and internally originating thermal "noise" power is given by

$$\Delta T_a = (T_e + T_A)\left(\frac{8b}{B}\right)^{1/2} \quad (6)$$

Where: T_e is the excess noise temperature of the receiver

T_A is the total antenna temperature

B and b are the pre and post detection bandwidths respectively.

Equation (6) expresses the radiometric system noise in terms of an equivalent RMS fluctuation of the apparent antenna temperature.

The radiometric signal to noise ratio from Equations (5) and (6) is:

$$S/N = \frac{T_a}{\Delta T_a} \quad (7)$$

It should be noted that the radiometric signal to noise ratio includes the effects of thermal noise both internal and external to the receiver. Referring to Equation (6) the system is background limited when $T_A >> T_e$. In most practical cases involving terrestrial surface sensing $T_e \geq T_A$. The radiation frequency selectivity of monochromaticity of the receiver is expressed by the quantity B. The data bandwidth is expressed by b. The incoming radiation intensity is measured quantitatively by periodic comparison of the antenna radiation temperature against transmission line black bodies at known reference temperatures.

ELECTRONICALL SCANNED MICROWAVE IMAGER

The current state of the art in microwave radiometric imaging is exemplified by a system developed for NASA by Aerojet-General Corporation. It is a prototype microwave radiometric imager for future application in the NIMBUS Meteorological Satellites. This system employs a 19.35 GHz solid state superheterodyne receiver together with an electronically scanning phased array antenna. A simplified block diagram of the imager is shown in Figure 9. A photograph of the equipment together with pertinent system parameters is given in Figure 10. The antenna beam is circular and has a diameter of 2.8^o. When the imager is mounted in an aircraft or space vehicle this beam is scanned $\pm 50^o$ in a plane transverse

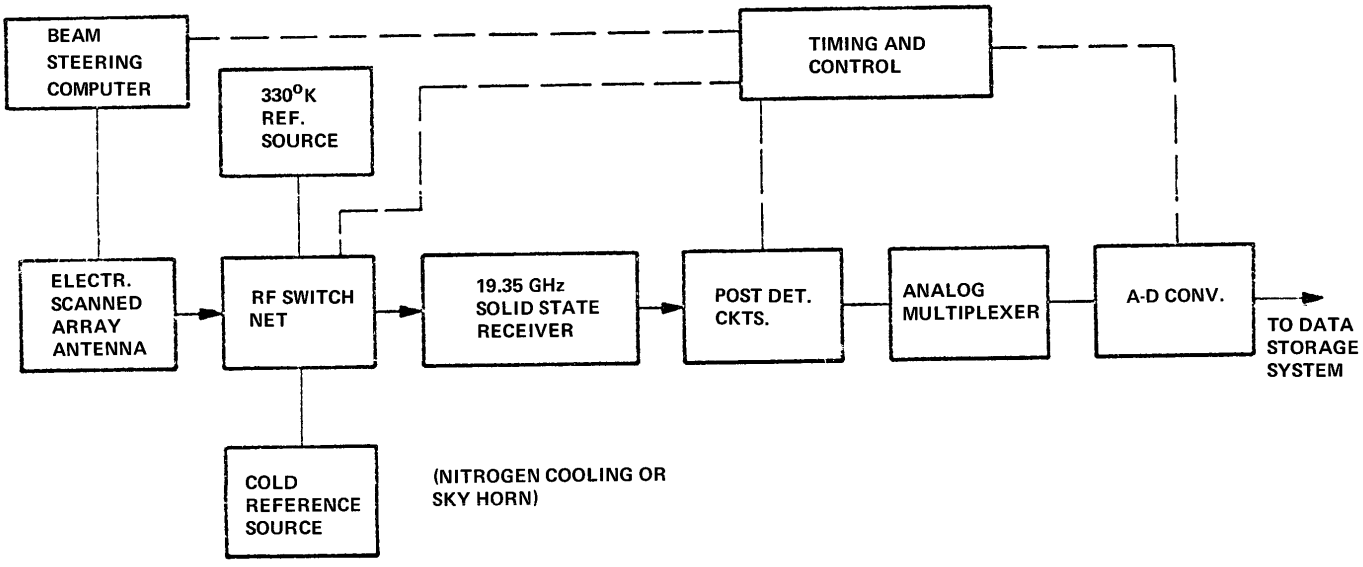

Figure 9. Electronically Scanned 19.35 GHz Radiometer Block Diagram (Wavelength = 1.55 cm)

Approved For Release 2004/02/11 : CIA-RDP78B05703A000100070021-5

PASSIVE 19.35 GHz ELECTRONICALLY SCANNED MICROWAVE IMAGING SYSTEM

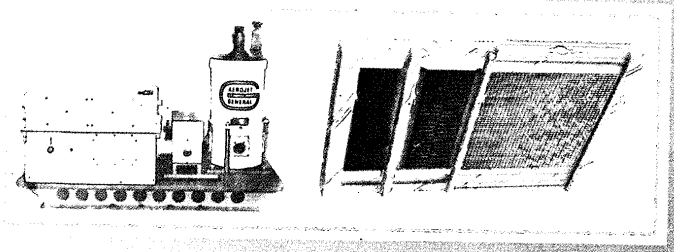

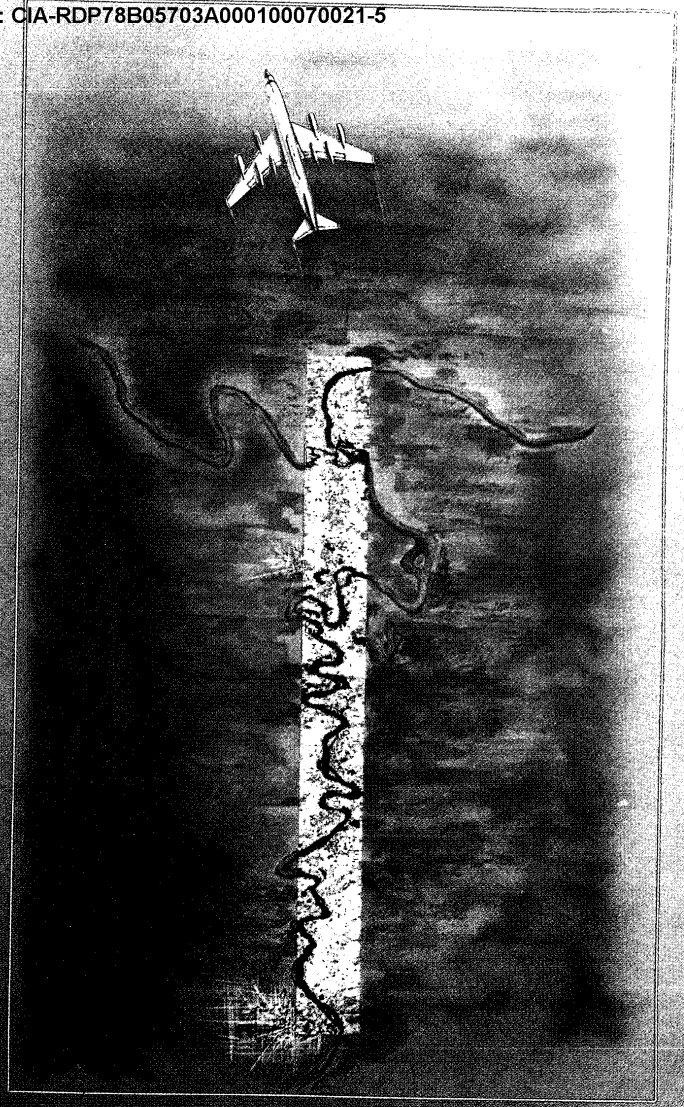

THE 19.35 GHz IMAGING RADIOMETER IS A SMALL, LIGHTWEIGHT, ELECTRONICALLY SCANNED PASSIVE MICROWAVE SYSTEM DEVELOPED FOR SPACE-BORNE OR AIRBORNE APPLICATION. CONVENTIONAL EDGE-SLOTTED TRAVELING-WAVE LINEAR ELEMENTS ARE ASSEMBLED INTO A PLANAR ARRAY WHICH SUBTENDS A DIRECTIONAL BEAM. THIS BEAM IS SCANNED BACK AND FORTH IN ONE DIMENSION BY FERRITE PHASE SHIFTING ELEMENTS. THE SECOND DIMENSION OF THE SCAN IS PROVIDED BY THE AIRCRAFT OR SATELLITE AS IT PASSES ACROSS THE EARTH'S SURFACE.

THE IMAGE IS OBTAINED FROM A DIGITAL TAPE THAT IS RECORDED DURING FLIGHT. THE TAPE IS PLAYED BACK ON A COMPUTER AND USED TO DRIVE A COLOR CRT SYSTEM TO PRODUCE AN IMAGE. EACH TEMPERATURE INCREMENT IS REPRESENTED BY A COLOR SHADE. HIGHER RADIOMETRIC TEMPERATURES APPEAR AS LIGHTER COLORS, WHITE BEING THE WARMEST. THE IMAGERY DERIVED FROM THE CRT IS PHOTOGRAPHED AND PRESENTED IN TIME SEQUENCES.

CHARACTERISTICS

ANTENNA	49 ELEMENT 36 SLOT PHASED ARRAY
SCANNING	ELECTRONIC
RECEIVING APERTURE	14.35" X 15.84"
FREQUENCY	19.35 GHz
ANGULAR COVERAGE	±50°
STEPS PER SCAN (BEAM POSITIONS)	39
SCAN TIME	1 SEC-FAST 2 SEC-SLOW
BEAM WIDTH	2.6°
MEASUREMENT ACCURACY	2° K

Figure 10. Passive 19.35 GHz Electronically Scanned Imaging System

to the flight direction. This results in a strip map whose width is proportional to the product of the altitude and scan angle. An artist's concept of the radiometric strip map superimposed on the terrain is shown in Figure 10. The beam scanning is executed in a step wise fashion through 39 positions with adjacent beam positions overlapping at the half power points. The radiometer output corresponding to each beam position defines the apparent microwave brightness temperature of a specific elemental circular area on the surface. The diameter of this area is the product of altitude and the antenna beamwidth. The period of the scan is determined by the time in which the vehicle moves forward by one surface element diameter. The measurements of the individual area elements are made with respect to a temperature controlled transmission line reference source. The radiometric gain calibration, i.e., output voltage versus temperature scale is checked at the end of each scan. This calibration is effected by measuring the system response to a cold reference body substituted for the antenna. This provides a temperature scale which permits the measurements with an absolute accuracy of $2^{o}K$. The radiometer output, as well as various "internal housekeeping functions" are time multiplexed and converted in a digital format shown in Figure 11.

Photographs of the equipment are seen in the upper left of Figure 10. The rectangular white box with dimensions of approximately 12" x 12" x 18" houses the solid state radiometer, the antenna beam steering computer, the digital timing and control networks together with the telemetry interface circuits. Mounted immediately to the right on the same pallet or support structure employed in aircraft operation is an external cryogenically cooled reference black body. It consists of a waveguide transmission line termination in an evacuated cryoflask cooled with liquid nitrogen. This external radiation reference at $78^{o}F$ is substituted for the antenna at the end of each scan. As mentioned above, the radiometer gain scale is calibrated using this external cold reference and the internal hot reference.

The planer array antenna is shown to be right of the cryogenic reference source, the antenna aperture is approximately 15" x 15". The antenna is composed of 49 linear arrays consisting of edge slotted waveguide transmission lines whose axes are parallel and coplanar. The spacing between these linear arrays is approximately one-half wavelength. Each linear array element has 36 radiating orfices in the form of edge slots spaced at half wave

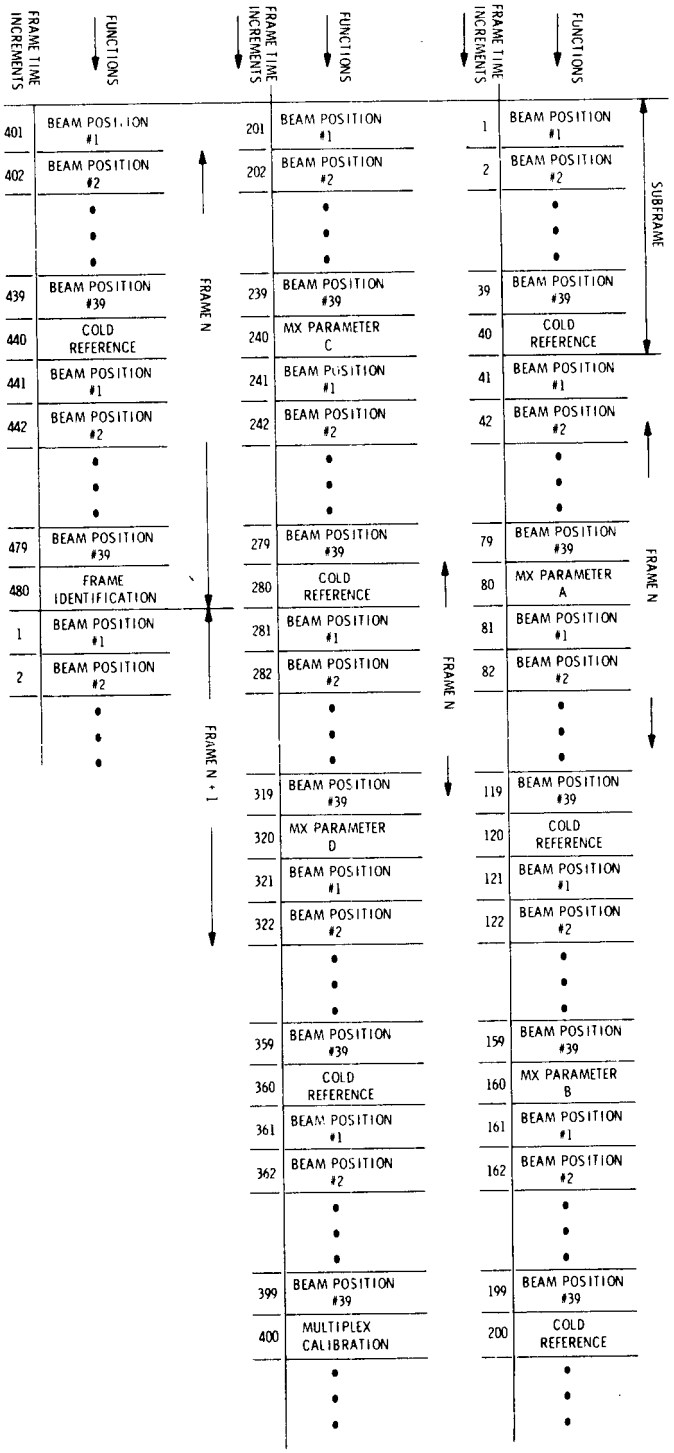

Figure 11. Imaging Radiometer Digital Framing Format

intervals. Thus, the planar conducting surface of the array contains approximately 1800 radiating elements spaced approximately at half wave intervals in both directions.

The radiation received by each of the 49 individual linear arrays is collected by a summation transmission line whose output connects to the radiometer. Between the summation line and each of the individual 49 linear arrays there is a microwave phase shifter. The relative phase shift between adjacent linear arrays controls the position of the antenna beam in the plane normal to the axes of the linear arrays. The microwave phase shifters consist of tapered thin ferrite cylinders mounted axially in the waveguide transmission line. The microwave phase shift introduced by the ferrite medium is determined by the external magnetic field imposed by the current flow in the solenoids wound externally around the waveguides. For a given position of the antenna beam there is a given set of 49 currents for the 49 phase shifters. In this case where there are approximately 39 discrete beam positions 39 sets of current are sequentially generated by the beam steering computer in the course of each scan. A total of 1920 separate and precisely determined currents required during the scan are derived from a precision resistance matrix. This system, completed in 1967, has been operated by NASA, GSFC in a Convair 990 aircraft in a variety of scientific missions. (Ref. 7) In the aircraft operating mode, the digitized data is recorded on magnetic tape and is also presented in real time on facsimile machine. The magnetic tape record is used with appropriate computer processing to take into account in flight calibration of the radiometer, as well as known antenna characteristics and geometric corrections in order to produce a two-dimensional strip map showing the surface distribution of brightness temperature at the 1.55 cm wavelength. The dynamic range of the measurement covers approximately 200^{o}K while the system is capable of 1^{o}K resolution. The corrected output at the ground based data processing center can be numerically printed out on paper in 1^{o}K increments. However, this does not provide a spatial pattern configuration most suitable for the data interpretation. A two dimensional intensity modulated display is very useful in that it clearly presents spatial distribution patterns. An eight gray level real time display is employed in the aircraft. An improved display providing greater dynamic range and resolution of brightness temperatures is achieved by using a color coded display. It is implemented by converting the finalized corrected radiation intensities into analog amplitudes controlling the intensities of a color TV tube display in such a fashion as to achieve a color scale corresponding to radiometric brightness temperature. In addition to brightness, hue and saturation provide two additional controlled parameters. Color moving picture film strips and color still shots of the TV tube display constitute permanent records of the color display. The same magnetic tape can be reprocessed numerous times to obtain a variety of different color processing effects enhancing certain aspects of the microwave radiometric image.

REMOTE SENSING APPLICATIONS

The capability for all-weather observation unimpaired by clouds and rain makes microwave radiometric remote sensing very useful in complementing existing visual and infrared sensors. Extensive measurements have demonstrated, uniquely, distinctive microwave signatures for physical features of particular significance in earth resources and meteorology investigations. (Refs. 8, 9, 10, 11) Earth resources investigations from satellites and aircraft include the following areas:

1. Water Resource Surveys and Management.

Geographical distribution and its seasonal variations for the following:

   a) Soil moisture and drainage basin monitoring.

   b) Ice and snow accumulation.

   c) Snow moisture content.

2. Polar Ice Monitoring

3. Sea State

4. Mapping of Rain Distribution

5. Temperature Profiling of Upper Atmosphere.

Especially for remote sensing of soil and snow moisture content, microwave radiometric techniques provide signatures for which no counterpart exists in the visual and infrared spectrum. Microwave signatures permit discrimination between ice and water not only on basis of intensity but also on basis of polarization. This provides considerable advantages for mapping of ice distribution in the arctic regions.

The practical utilization of these microwave characteristics requires reliable operational imaging equipment and data processing techniques. The above mentioned 19.35 GHz radiometric imager demonstrates this capability. The following examples of radiometric images made from a high altitude jet aircraft illustrate results obtained to

date. They are photographic reproductions of microwave radiometric maps in which the various individual color values correspond to specific levels of microwave brightness temperature. In the typical case, the brightness temperature range extends from approximately 150°K to 300°K with a corresponding color scale extending from dark blue through to light red at the hot end of the scale. In practice, it has been found possible to establish synthetic color scales with as many as fifty distinguishable colors each corresponding to a specific value of radiometric brightness temperature.

These radiometric maps made by means of 1.55 cm wavelength radiation provide maximum contrasts for water - land boundaries. This fully confirms theoretical expectation. The maps clearly demonstrate the capability to accurately delineate the geographical distribution patterns of water resources in all forms.

Urban areas with their associated expanses of specular surfaces in general are shown to have low values of brightness temperature when viewed at centimeter wavelengths. The regions indicated to be the warmest are those covered with heavy vegetation.

A significant aspect of the data processing employed in the production of the color coded radiometric maps is the selection of the proper scale factors and upper or lower temperature thresholds. These selections ideally are made so as to maximize the contrast of a particular surface feature against the overall background.

The radiometric map of the St. Louis, Missouri area shown in Figure 12, is especially interesting. It dramatically demonstrates the ability of microwave radiometric sensing to provide images of areas underlying heavy cloud cover. The courses and junction of the two rivers are clearly defined. The urban regions also show up quite distinctly.

The potential for the detection and measurement of sea state conditions is illustrated in Figure 13. It shows the brightness temperature distribution on the Salton Sea in Southern California. At the time of observations, there were heavy winds and large wave conditions at the southern end while the northern end was relatively calm. The heavy sea areas as indicated by elevated microwave brightness temperature conformed with the visually observed distribution. This provided an excellent confirmation of results anticipated on basis of previous theoretical work. The effects of alternate processing procedures in enhancing contrast is shown in the same figure. As would be expected, the expanded scale over a more restricted dynamic range provides a more marked contrast and fine structure detail regarding the distributions of brightness temperature of the sea surface. Since these are centered in the vicinity of 150°K the land temperatures are beyond the high end of the scale at 195°K. It is interesting to note that even with the extended range with 4.5°K steps, the overall pattern of the sea state distribution is clearly discernible.

In Figure 14, another example is shown of how data processing is applied to enhance contrast and extract specific features from the total data output of the radiometric sensor. These moderate changes in the temperature quantitization and the location of the upper threshold effect a marked improvement in the discrimination of the radiometrically cooler canal and city from the remaining background.

In summary, these maps illustrate the types of terrain feature signatures obtained with microwave radiometric instrumentation. They represent the results of initial effort and should be considered indicative of the potential for further evolution in the instrumentation technology. Second generation imagers now in development will provide an order of magnitude more resolution cells per unit surface area. Additionally, the application of more advanced methods of sampling and spatial filtering will be applied to achieve further improvements in effective resolution. These latter efforts will tend to reduce the relatively granular nature of the present maps.

FUTURE DIRECTIONS

The demonstrated practicality of airborne microwave radiometric imagers provides the impetus to the development of advanced systems for both satellite and airborne operation.

An advanced version of the previously described 1.55 cm wavelength system is presently being developed at [redacted] for NASA Goddard Space Flight Center. This system, to be employed in the forthcoming Nimbus Satellites, will employ a 1° antenna beamwidth. In comparison with the previous imager the number of area resolution elements is increased by an order of magnitude. The resulting data rate is increased accordingly. The improved area resolution results from

25X1

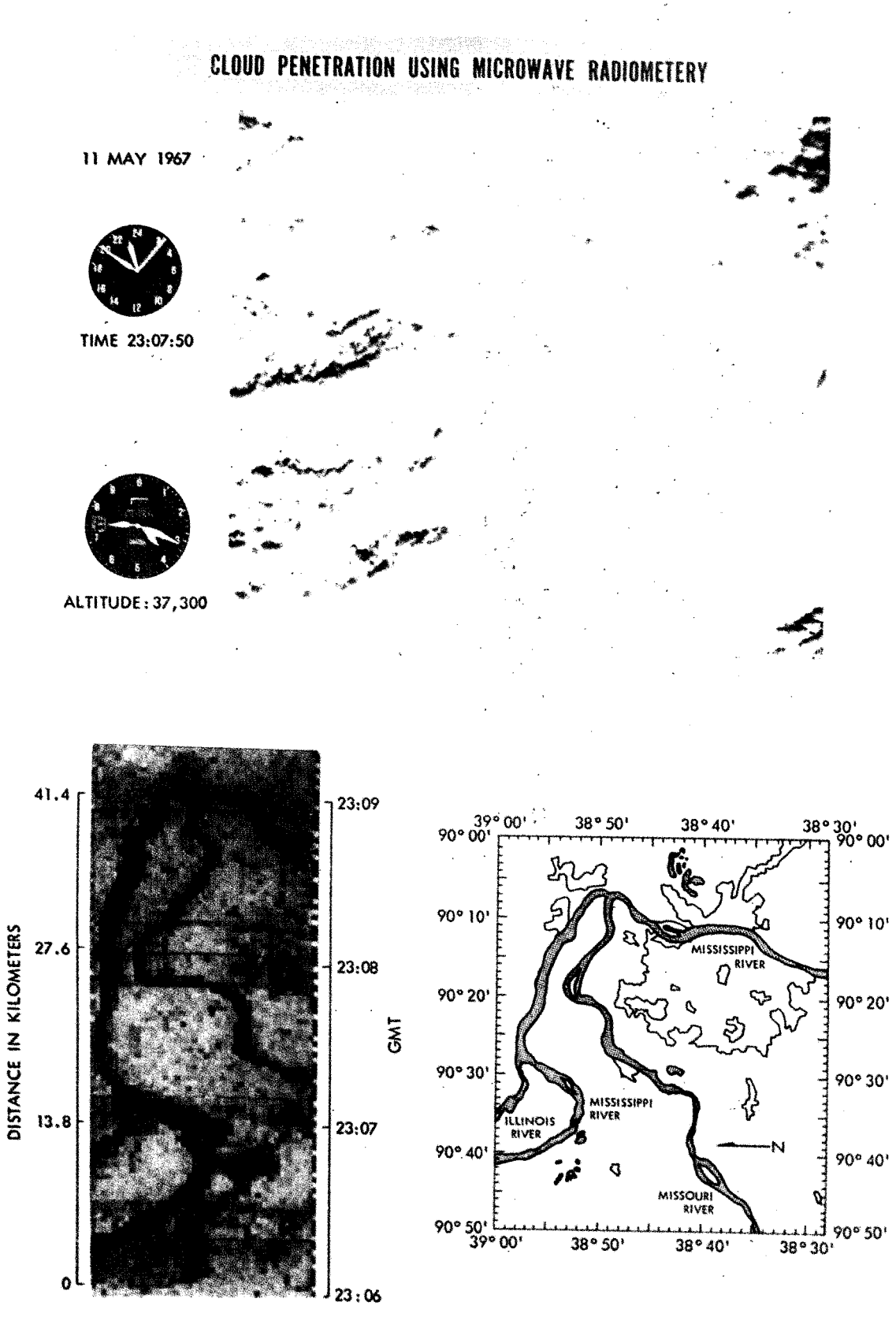

Figure 12. Radiometric Map of St. Louis Area Through Heavy Cloud Cover

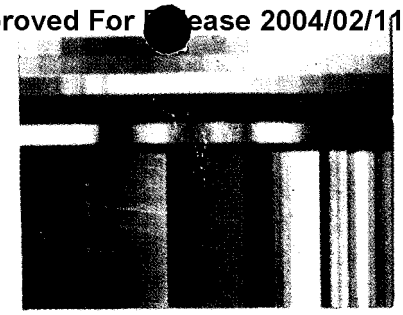

WHITE HOTTEST

BLACK - COLDEST

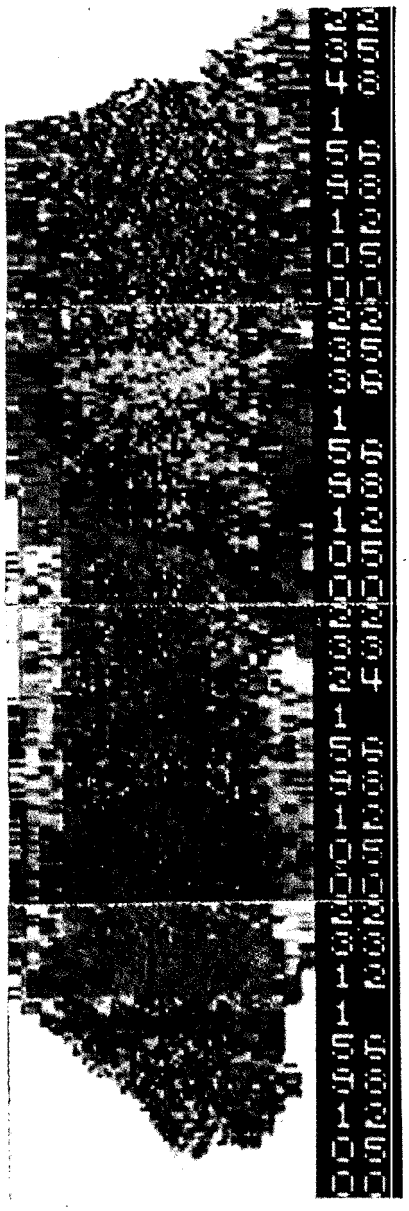

WHITE ≥ 195°K
BLACK ≤ 119°K
°K/COLOR = 1.5

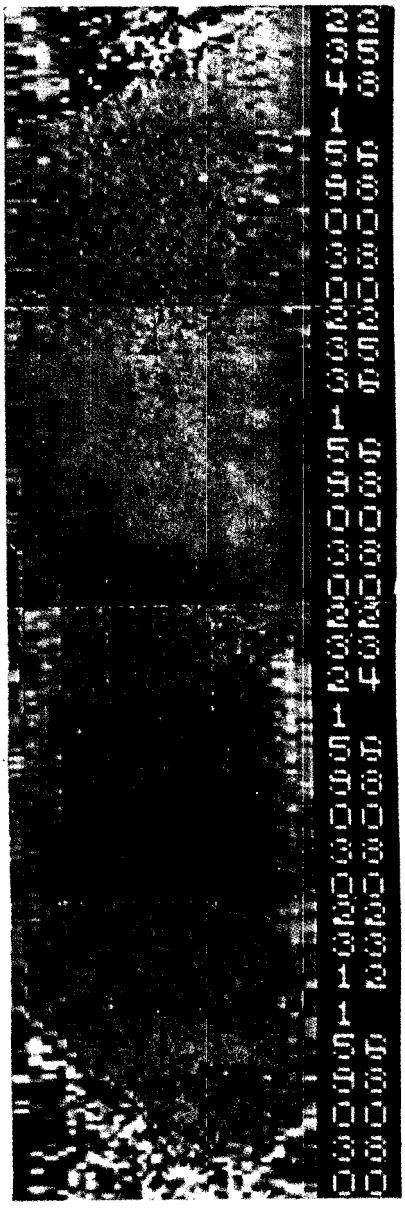

WHITE ≥317°K
BLACK ≤ 67°K
°K/COLOR = 4.7

FLIGHT DIRECTION WAS FROM NORTH TO SOUTH, THEREFORE THE SOUTHERN END OF THE SEA IS AT THE TOP OF THE SEQUENCE. FRAME 22:35:36 SHOWS A MARKED DIFFERENCE IN RADIOMETRIC TEMPERATURE OF THE SEA SURFACE WHICH CORRESPONDS TO HIGHER SEA STATE IN THE SOUTHERN HALF OF THE SEA.

advances in antenna design. The increased time rate of data with the same or better resolution in brightness temperature magnitudes will be achieved by significant reductions of the internal noise levels of the microwave receiver.

A significant trend in airborne systems for earth resources remote sensing is the use of multi-wavelength instrumentation. An example is the system recently placed in operation by NASA - Manned Spaced Flight Center. The system consists of four precision calibrated microwave radiometers operating at wavelengths of 21.2 cm, 3.2 cm, 1.34 cm and 0.95 cm. The 1.34 cm radiometer incorporates two data channels at two slightly different wavelengths. One wavelength exactly equal to that of the water vapor resonance line while the second is slightly displaced from resonance. In this manner, the radiation contributions of atmospheric water vapor are evaluated and a more accurate reading of surface brightness temperature is achieved.

An airborne imager providing simultaneous presentation of both the horizontal and vertical components of brightness temperature in the 3 cm wavelength region

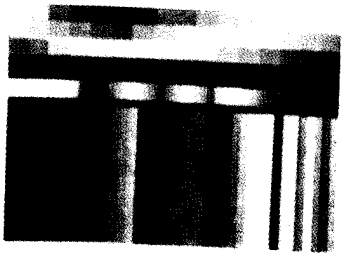

WHITE = HOTTEST

BLACK = COLDEST

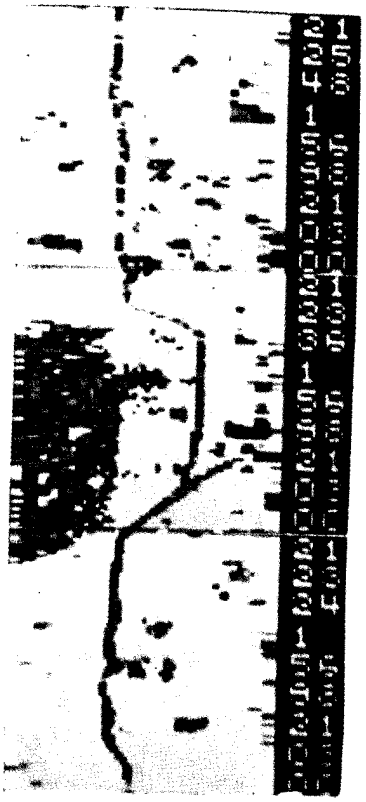

WHITE ≥ 281°K
BLACK ≤ 245°K
°K/COLOR = 0.7

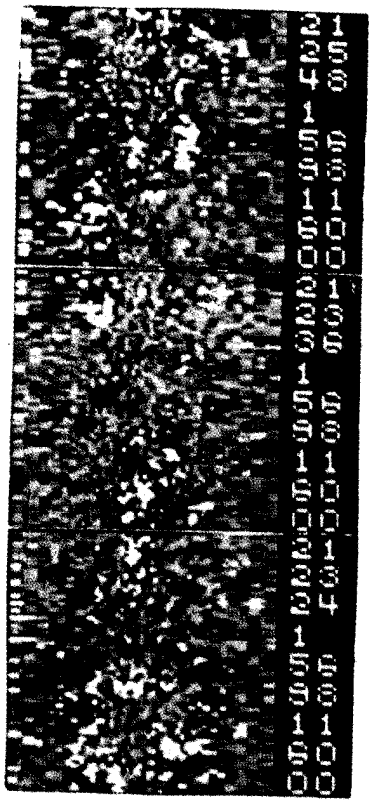

WHITE ≥ 304°K
BLACK ≤ 256°K
°K/COLOR = 1.0

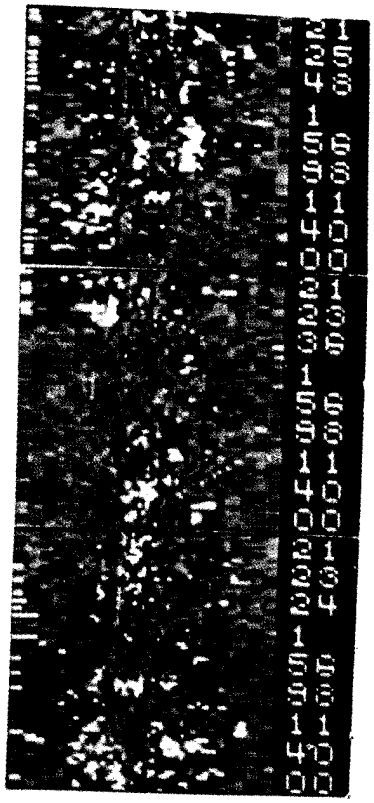

WHITE ≥ 304°K
BLACK ≤ 249°K
°K/COLOR = 1.1

RADIOMETRICALLY COOLER AREA IN FRAME 21:23:36 CORRESPONDS TO THE CITY OF MEXICALLI, MEXICO.

Figure 14. Radiometric Image Showing All American Canal Along U.S. - Mexico Border

is presently being developed for NASA Manned Space Flight Center by [redacted] 25X1

In addition to digital recorded magnetic tape data records a real time airborne color code display will be employed. The computer controlled color cathode ray tube display will simultaneously provide horizontal and vertical brightness temperature images. These real time displays together with visual and infrared displays will be a major asset to scientific investigators in the conduct of their experiments.

A ground based computer installation specifically designed to correlate microwave and multi-wavelength infrared data will be employed. The acquisition, interpretation, and correlation of multispectral data ranging from visual through the centimeter wavelength region appears to be the dominant trend in the evolution of future remote sensing systems.

CONCLUSIONS

Fundamental physical considerations show that microwave passive sensing offers a great potential to complement visual and infrared sensors. The numerous investigations indicate many specific applications for microwave sensing. Recent developments in microwave radiometric imaging instrumentation technology permit the realization of these applications. Advances in data processing and data interpretation will require increased emphasis in the future. 25X1

[redacted]

REFERENCES

1. Medhurst, R. G., "Rainfall Attenuation of Centimeter Waves: Comparison of Theory and Measurement", IEEE Transactions Antennas & Propagation AP-13 No. 4 550-564 (1965)

2. Wilson, R. W., "Sun Tracker Measurements of Attenuation by Rain at 16 and 30 GHz. Bell System Technical Journal, 1383-1404 May-June 1969.

3. Dicke, R. H. et al, "Cosmic Black Body Radiation", Astrophysic Journal Vol. 142 pp. 414-479, 1965.

4. Stogryn, A., "The Apparent Temperature of the Sea at Microwave Frequencies" IEEE Transactions on Antennas and Propagation Vol. AP-15 No. 2 March 1967.

5. Nyquist, H., "Thermal Agitation of Electric Charge in Conductors", Phys. Rev. Vol. 32, pp. 110-113, 1928.

6. Dicke, R. H., "The Measurement at Thermal Radiation at Microwave Frequencies" Rev. Sci. Instr. Vol. 17, pp. 268-275, July 1946.

7. Nordberg, W. et al, "Preliminary Results from Aircraft Flight Tests of an Electronically Scanning Microwave Radiometer" NASA Goddard Space Flight Center Report X-622-67-352.

8. Pascalar, H., "Microwave Radiometric Measurements of Ice and Water", Proceedings of Third Symposium on Remote Sensing University of Michigan, October 1964.

9. Kennedy, J., Sakamoto, R., "Passive Microwave Determination of Snow Wetness Factors", Proceedings of Fifth Symposium on Remote Sensing, University of Michigan, April 1966.

10. Kennedy, J. Edgerton, A., "Microwave Radiometric Sensing of Soil Moisture Content" 14 General Assembly International Union of Geodesy and Geophysics, September 1967.

11. Edgerton, A., et al, "Passive Microwave Investigations of Snow, Soils and Snow-Ice-Water Systems, Aerojet-General Corporation Report, Feb. 1968.

ACL

Senate Space Unit Restores Part of NASA Budget Cut

Washington–Senate space committee last week voted a net increase of more than $119 million in the National Aeronautics and Space Administration Fiscal 1969 budget passed by the House. The Senate is expected to approve the action.

The total $4.15 billion recommended by the Senate committee compared with $4.03 billion previously voted by the House (AW&ST May 13, p. 35). NASA asked $4.37 billion.

The Senate group approved $2.025 billion for the Apollo program. This is the same amount voted by the House, and only $13.8 million below NASA's request.

The additions voted by the Senate space committee were:

- **Apollo Applications,** $96.8 million. The $350 million approved would still be $89.6 million below NASA's request.
- **Nuclear rocket,** $43.3 million. This would bring the total allocation to $55 million, $5 million less than NASA asked. The $11.7 million allowed by the House would mean cancellation of the program for development of the 75,000-lb.-thrust Nerva 1 engine for a Saturn 5 third-stage.
- **Administrative operations,** $32.4 million. The House reduced the $648 million NASA asked by more than $45 million.
- **Bioscience** program, $6 million. This would bring the total allocation to $39.3 million, still $9.2 million below NASA's request.
- **Launch vehicle** procurement, $2 million. The $118 million allowed is $10.6 million below NASA's request.

Partially offsetting these additions totaling more than $180 million were reductions of $61.3 million made by the Senate committee. The reductions were:

- **Lunar and planetary** exploration, $10.1 million. Added to the $4.9-million reduction by the House, this would leave $92.3 million.
- **Space Applications,** $13.5 million. The House voted the full $112 million asked.
- **Space vehicle** systems, $3.5 million. The House allowed the full $35.3 million requested for this broad-based research and technology program.
- **Electronic systems,** $3.9 million. The House approved the $39.4 million requested.
- **Chemical propulsion,** $6.5 million. The House approved the full $36.7 million requested.
- **Aeronautical program,** $3 million. The House approved a $77.9-million program, adding $1 million to NASA's request.
- **Data and tracking,** $10 million. Added to a $5-million House reduction, this would leave an allocation of $289 million, compared with the $304 million requested.
- **Construction,** $5.4 million. The House approved the full $45 million requested.

The Senate space committee also made these smaller reductions: physics and astronomy, $1.25 million; sustaining university program, $1 million; human factors, $2 million; basic research, $1 million, and technology utilization, $200,000.

House-Senate differences in the budget authorization will be compromised by conferees of the two houses.

In passing the NASA appropriation, the House made only one change in the amounts previously passed in the authorization. This was a reduction of $23.2 million from the $45 million previously authorized for construction.

X-14 System

Northrop Corp.'s Norair Div. will produce a variable stability system to extend the flight simulation capabilities of the Bell Aerosystems X-14 V/STOL aircraft.

National Aeronautics and Space Administration's Ames Research Center has contracted with Norair for installation of an on-board digital computer to provide variable flight stability in the X-14.

Airborne Radiometer Yields Resource Data

Greenbelt, Md.–Microwave observations of earth surfaces from an aircraft are producing valuable data on thermal radiation with potentially far-reaching effects upon worldwide natural resources.

A small percentage of the observations made to date is reproduced on the cover of this issue of AVIATION WEEK & SPACE TECHNOLOGY.

The photographs were taken from a Convair CV 990 jet aircraft operated by the National Aeronautics and Space Administration. Microwave radiation experts at NASA's Goddard Space Flight Center here are analyzing the results.

Thermal radiation emitted from the earth's surface at a 1.55 cm. wavelength was received by an electrically scanning microwave radiometer operated under NASA contract by the Space Div. of Aerojet-General Corp. William Nordberg, a project scientist at Goddard, is in charge of the analysis.

In the photographs reproduced on the cover, each of the color strips (five full strips and portions of two others in each of the three sections) represents a ground width of 10 mi.

Each of the individual color squares, or resolution elements, represents an area 1,500 x 1,500 ft. The CV 990 flew at an altitude of about 37,000 ft., along the center of each strip.

There are 32 shades of color, corresponding to 32 discrete, equivalent temperature values ranging from dark blue at the coldest end of the spectrum to white where the emissivity is warmest.

The strip on the top of the cover was taken from segments obtained over forested areas of eastern Kentucky and western Virginia in late afternoon.

The sun had been shining and the terrain was relatively warm. The highest radiation temperatures, as a result, were obtained here and are reflected by the purple and white resolution elements.

The cold, or light blue, region at the left corresponds to the city of Lexington, Ky. Nordberg explained that the lower emissivity of man-made structures and concrete compared to vegetation results in the lowered brightness temperatures.

The middle strip was taken from radiation emitted from farmland in the mid-western U.S.

The flight path was from east to west about 20 mi. north of Evansville, Ind.

Freshly plowed fields, whose emissivity is markedly lower than that of heavily overgrown land, appear colder, or light blue, than vegetated areas which show up—depending on the amount of vegetation—as yellow or red.

Observations in the lower composite were made over St. Louis, Mo., and show the confluence of the Mississippi and the Illinois rivers (in the second complete strip from the left) and of the Missouri River with St. Louis, at the lower right.

Brightness temperature of the rivers and wet banks is extremely cold and is dark blue because of the low thermal emissivity in the microwave spectrum. Moist land is somewhat lighter blue. Dry, vegetated land has a high emissivity and appears to be warmer.

Nordberg now is studying additional data taken from the CV 990 aircraft of ice flows in the North Atlantic to trace the movement of large ice masses. He also has obtained data on a considerable amount of the U.S. earth surface, including detailed thermal emissivity of the West Coast.

TECHNICAL BRIEF

Microwave Systems

COLOR DISPLAY SYSTEM

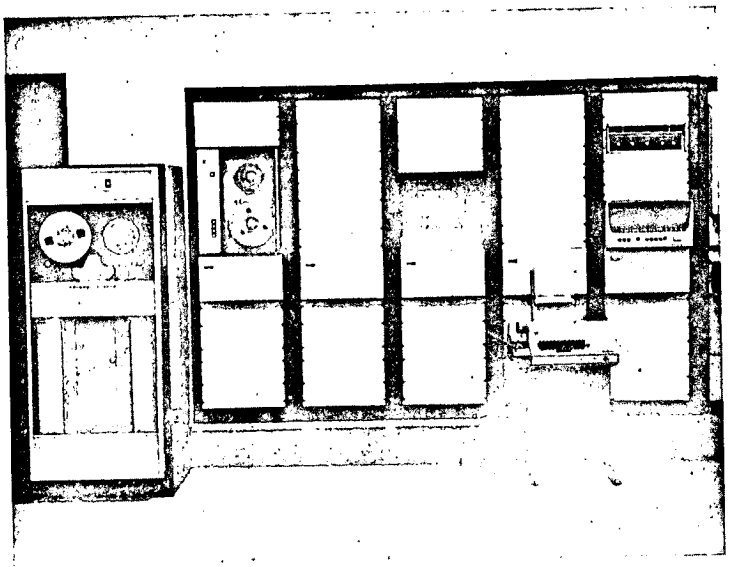

Several years ago the Space Division recognized the need, within the scientific community, for a display system that could accurately provide more than two dimensional information to an observer. At that time, the best available display system could portray data with a high degree of resolution and accuracy in two dimensions, but lacked resolution and accuracy in the third dimension.

25X1 [redacted] Space Division has developed a highly refined display technique which provides approximately 1% resolution and accuracy in two dimensions and at least 2% resolution and accuracy in the third.

The display technique uses X and Y displacement to describe two dimensions and various combinations of color hue, saturation and luminescence of the three primary colors to display the third dimension. Work to date has

shown that the visual acuity of the human eye can discern, on an absolute basis, over fifty different combinations of color hue, saturation and luminescence. It also appears that fifty different color values do not represent the limit of the detection capability of the human eye. Previously, three dimensional presentations provided only changes in luminescence levels to indicate the magnitude of the third dimension. The human eye most readily resolves boundaries between luminescence changes but the eyes ability to detect absolute luminescence magnitudes limited from 4 to 6 different shades of gray.

The color display system may be programmed to provide as many as 512 different combinations of color hue, saturation and luminescence to display the magnitude of the third dimension. The color display system will operate from replayed data for evaluation of different combinations of color presentations. The system is installed in [redacted] where complete facilities are available for the playback of previous recorded sensor data. 25X1

Key Features:

- Presentation of three dimensional information with high resolution and accuracy
- Rapid translation of large volumes of data
- Convenient manipulation of all three axis information to correct, compensate, or distort the displayed values.
- Real time or hard copy presentation of the displayed information
- Effortless changing of colors representing various magnitudes of input data

Application:

- Data analysis and reduction

25X1

[redacted]